

Impact of NaCl concentration in crystalline nanocellulose for printed ionic dielectrics

Elizabeth G. Franklin¹, Brittany Smith², Aaron D. Franklin^{2,3}

¹ Panther Creek High School, Cary, North Carolina

² Department of Electrical and Computer Engineering, Duke University, Durham, North Carolina

³ Department of Chemistry, Duke University, Durham, North Carolina

SUMMARY

While electronics continue to be an integral part of nearly every aspect of our lives, there is a growing need for more environmentally friendly electronic materials and manufacturing processes. The use of crystalline nanocellulose (CNC) as a biodegradable dielectric material has recently gained interest due to its high capacitance at low voltages and compatibility with additive manufacturing techniques, such as printing. The addition of salt to the CNC has shown improved performance in transistor applications, but a thorough study optimizing the addition of NaCl in CNC capacitors has not been completed. We hypothesized that increasing the NaCl concentration altered the charging characteristics of the CNC. In this work, we verified this hypothesis by measuring the charging and discharging characteristics for CNC capacitors with varying NaCl concentrations and extracting the resistance-capacitance (RC) delay and charging current. These aerosol jet printed capacitors consisted of graphene top and bottom electrodes and a CNC dielectric sandwiched between the electrodes. The results reveal a minimum charging current at a NaCl concentration of 0.05%, independent of the applied voltage, and a minimized RC delay at NaCl concentrations above 0.1% with applied voltages below 2 V. These findings show that there are trade-offs that must be managed between RC delay and charging current, thus the NaCl concentration must be optimized for each application. This work is another significant step in understanding the electrical properties of CNC so that this environmentally friendly material may one day be utilized in commercially available electronics.

INTRODUCTION

Transistors have enabled the technological revolution through the discovery and use of semiconducting materials. These devices helped bring computers from filling an entire room in the 1960s to the sleek, thin laptops we know today (1). Silicon transistors are everywhere, including in phones, watches, and displays. Due to the ongoing research and development of transistors, the number of transistors on a chip has roughly doubled every two years since its inception, an observation called Moore's law (2). Since the current demand for transistors is rising, so is the environmental cost. While each individual transistor may be only a few nanometers in size, there may be over 100 billion of them on each integrated

circuit or chip, such as the Apple M1 chip released in 2021 (3). Given how widespread chip technology has become, the e-waste of these devices has a large ecological footprint (4). Silicon itself, being difficult to recycle and non-biodegradable, is not a sustainable material, which warrants research efforts into new materials for transistors (5-6).

What if there were materials that could replace silicon in transistors and also be recycled and/or safely biodegraded? Recent results show promise for using printed electronic nanomaterials for recyclable and biodegradable electronics (7-8). One of these nanomaterials is crystalline nanocellulose (CNC), which is extracted from plant fibrils and therefore is a carbon-based substance that is completely biodegradable (9-10). CNC can be used as a binder to enable the printing of other materials, as a substrate for supporting printed electronic circuits, or as a standalone printed ionic dielectric. Since CNC has only recently been used as a standalone dielectric, there is limited understanding regarding how the material performs electrically. Dielectrics are insulating materials that are crucial in transistors; they separate the semiconductor and metal gate, allowing the device to work like a switch. Ionic dielectrics are attractive for use in printed electronics because they enable operation of printed transistors at low voltages (11-13). However, their operation is also strongly dependent on ionic concentration and thus their formulation into printable inks requires optimization.

In this work, we studied the influence of salt concentration on the performance of printed ionic CNC dielectrics. We hypothesized that an increased salt concentration in the CNC film would increase the charging current of the capacitor (i.e., the ion current within the CNC to reach peak capacitance) and reduce the RC delay by providing more ions to form the electric double layers. To understand the influence of the salt content on dielectric performance, we printed the CNC with NaCl concentrations by weight ranging from 0 to 0.2 % into sandwich-style capacitor structures with printed graphene as the bottom and top electrodes. All printing was performed using an aerosol jet printer. The capacitor structures were used to test the charge/discharge behavior of the CNC using a variety of fixed charging voltages, ranging from 0.05 to 2 V. Our hypothesis was supported by the experimental findings, with the exception of CNC devices with a 0.05 % NaCl concentration under a 2V applied bias, which deviated slightly from the observed typical trend. These findings provide important insights for optimizing the formulation of CNC inks for a biodegradable, printed ionic dielectric.

RESULTS

At their most basic level, transistors are switches that can either be on or off. When a transistor is on, current can flow through its semiconductor channel from source to drain; in the transistor's off-state, the semiconductor is no longer able to conduct as much current. Capacitors are the part of a transistor that allow for an applied voltage to switch the semiconducting material from on (conducting) to off (insulating) without supplying additional current to the device. A capacitor is composed of an insulating material, known as a dielectric, that is placed between two conducting materials. When a voltage is applied across the capacitor, the insulating material stops electric current from flowing between the electrodes. The applied voltage creates an electric field that enables charge to be stored in the capacitor. When the voltage is no longer applied, the charge dissipates from the capacitor, also known as discharging. While the voltage is still applied, the capacitor will continue to hold its charge.

For CNC dielectrics, which operate as ionic dielectrics, the insulator behaves differently from a standard dielectric. Rather than having dipoles in the material aligned to the applied electric field or the charging of conducting plates (as is the case in standard dielectrics), ions within an ionic dielectric migrate to the electrode surfaces – positive ions to the negative electrode and negative ions to the positive electrode. At the electrode interfaces with the ionic dielectric, charges build up on the electrodes to counter the ions, thus forming what is known as an electric double layer (EDL). This thin EDL provides a high capacitance that enables ionic dielectrics to operate at low voltage, making them very attractive for use in transistors (8). By changing the ionic concentration in these dielectrics, the performance can change since a higher ionic content will yield an increased ion current under an applied voltage. One method of changing the ionic concentration is by adding salt (e.g., NaCl), which dissociates into ions.

The capacitors in this study were fabricated using an aerosol jet printer on Kapton (or polyimide) substrates following a three-step process (Figure 1A). The first layer is a graphene bottom contact, then a CNC dielectric is printed on top (within this CNC dielectric are the different NaCl concentrations), and lastly a final layer of graphene forms a sandwich around the dielectric (14-15). The NaCl concentrations in the CNC ranged from 0 to 0.2%, with higher concentrations of NaCl unable to be printed due to high ink viscosity. We characterized the printed graphene and CNC layers in a scanning electron microscope (SEM), showing dense, pin-hole free printed films (Figure 1B-C). In the capacitor structure, voltage is applied to the top electrode referenced to the bottom electrode, which is grounded. Due to the high resistance of the printed graphene electrodes (~1 k Ω), no additional resistance was added in series with this capacitor, which is often required when performing this type of characterization (14).

To test these capacitors, we used a manual micromanipulator probe station connected to a source measurement unit (SMU) which applies different voltages to the capacitor and then records the response. First, 0 V was applied for about 10 seconds to ensure the capacitor was completely discharged. Next, a specific voltage was applied for 10 seconds. In this study, four different applied voltages were used to determine the influence of voltage on the

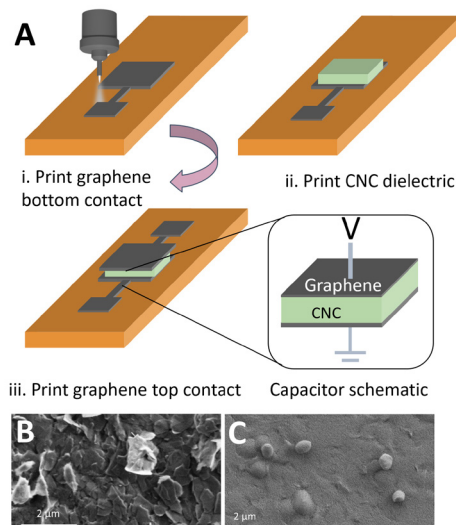


Figure 1. Printing process for CNC capacitors. A) Schematic of aerosol jet printing process for CNC capacitors, including printing of i) the graphene bottom contact on polyimide substrate, ii) the CNC ionic dielectric layer, and iii) the graphene top contact to complete the metal-dielectric-metal capacitor structure. SEM images showing detailed structure of printed B) graphene and C) CNC.

charging time, including 0.05 V, 0.1 V, 0.5 V, and 2 V. After the device was charged, the voltage was reduced back to 0 V for 10 seconds to allow for discharge, and then the process was repeated once more to ensure reproducibility (Figure 2).

From the charging and discharging curves, several capacitance characteristics may be extracted. The resistance-capacitance (RC) delay is the time at which the current decreases to 33% of the maximum current. We plotted RC delay versus voltage, showing a nearly linear increase in RC delay as voltage increases (Figure 3A-B). Further, we plotted RC delay versus NaCl concentration, revealing that the RC delay saturates at NaCl concentrations of 0.1% and 0.2% with applied voltages of 0.05 – 0.5 V. The maximum charging current (I) may also be measured and plotted versus NaCl concentration, highlighting that the charging current is highest at an NaCl concentration of 0.1% with an applied voltage of 2 V (Figure 3C).

DISCUSSION

In characterizing a capacitor, there are a few parameters that provide information about the quality of the insulating (dielectric) material and overall performance. The resistance-capacitance (RC) delay is a common measure of the performance for capacitor-related charging (14). A lower RC delay represents better performance as it enables the capacitor to be switched more rapidly between charged and discharged states. Reaching a charged state in a capacitor requires a charging current, which is related to the flow of ions to form an EDL in an ionic dielectric. The amount of charging current for an ionic dielectric is, in part, related to the concentration of ions, though there are other factors that can influence this parameter as well. Having a high charging and discharging current in a capacitor is typically related to having a low RC delay. Finally, the leakage current in a capacitor is from charge escaping from the electrodes through the

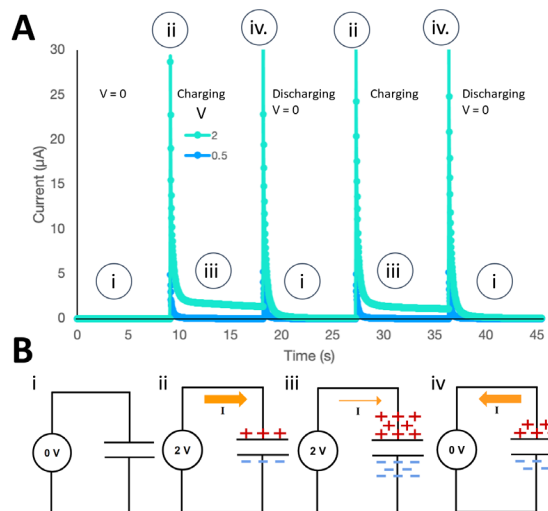


Figure 2. Charge and discharge characterization of printed CNC capacitors. A) Charging current versus time for a printed CNC capacitor with 0.05% NaCl concentration at voltages of 0.5 V and 2 V. **B)** Four distinct states of operation for the ionic CNC dielectric are illustrated in circuit schematics (i-iv), which depict ionic charge build-up and discharge based on applied voltage condition and history.

insulating dielectric – this is unwanted current, as an ideal dielectric would block all leakage current from flowing.

The charge and discharge current from a sequence of applied voltages is plotted in **Figure 2** for a printed capacitor using a CNC dielectric layer with an NaCl concentration of 0.05% at voltages of 0.5 V and 2 V. Before the charging/discharging cycle began, 0 V was applied across the capacitor so that any internal charge would be dissipated, resulting in no current going through the circuit (depicted in the small schematic i of **Figure 2**). When 2 V was applied across the capacitor, there was an initial spike in current corresponding to the flow of charge to build up at the CNC-graphene interface in response to the ionic charge in the CNC, forming the EDL at each interface (schematic ii of **Figure 2**). This initial spike in current dissipated quickly as the charge reaches a steady state in the EDL formation (schematic iii of **Figure 2**). The current not returning to zero after the charging of the EDLs was due to unwanted leakage current making its way through the CNC. This experiment shows us that a 2 V charging voltage creates more gate leakage than the 0.5 V, which is based on the larger electric field from the higher applied voltage. For the discharge cycles, when 0 V was applied, there was a similar spike in current to the charging cycle (schematic iv of **Figure 2**), but it was followed by a reduction to zero current once the EDLs were fully depleted of the built-up charge.

To test our hypothesis related to the impact of increased NaCl concentration in the CNC, the RC delay was measured at different charging voltages for capacitors using all four of the different concentrations of NaCl (**Figure 3**). As was hypothesized, the highest NaCl concentration produced the smallest RC delay of just over 70 ms (**Figure 3A-B**), which is low for an ionic dielectric but high compared to a traditional dielectric that does not depend on ionic current to reach a charged state. Importantly, it was found that the 0.1 % NaCl concentration produced nearly the same low RC as the maximum 0.2 % concentration, showing that there is a saturation point for realizing maximum benefit from the

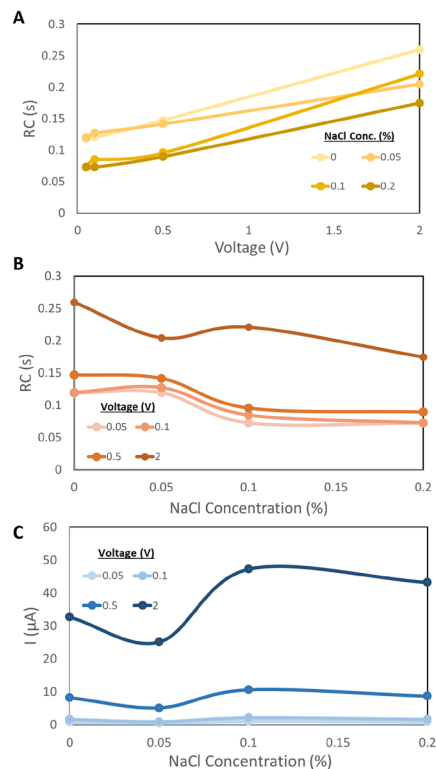


Figure 3. Electrical characterization of printed CNC capacitors. A) RC delay versus applied voltage for the four different NaCl concentrations in the CNC capacitors, verifying the RC delay increases with voltage. Impact of NaCl concentration on **B)** RC delay and **C)** current for four different applied voltages highlighting that increasing the applied voltage increases the charging current but also increases the RC delay. Spline curves added to guide the eye.

increased salt content.

All the studied NaCl concentrations produced the anticipated trend of increased RC delay with increased voltage (**Figure 3A**). This is attributed to an increase in resistance with voltage since the capacitance of ionic dielectrics is not highly dependent on applied voltage. At a NaCl concentration of 0.05 %, the data did deviate from the trends observed for the other NaCl concentrations, such as at an applied voltage of 2 V. This may be attributed to interactions with the sulfur and NaCl charges as they move through the material. The charging current corresponding to each of the NaCl concentrations is shown in **Figure 3C**, which revealed that the minimum current was reached at 0.05 % NaCl, independent of the charging voltage. Overall, the analysis of our results revealed that the RC delay is minimized at 72.4 ms at an NaCl concentration of 0.2 % and an applied voltage of 0.05 V. However, this low voltage may not yield a sufficient density of stored charge, and thus operation at 0.1 or 0.5 V may be more suitable for most applications. Overall, the CNC NaCl concentration may be optimized for specific applications.

Based on these findings, future experiments should study the impact of different nanocellulose types as well as surface groups, such as the sulfonic groups attached to the CNC in this study, on capacitor performance. This work will be crucial for understanding the role structure and surface groups play on dielectric performance. Further, a study on different electrical contacts on the RC time and peak discharging/

charging current would allow for the effects of graphene on capacitor performance to be observed. Since the graphene electrodes present the greatest series resistance of the device, a lower-resistance contact material, such as gold, will allow for the dielectric resistance of the CNC to be easily extracted along with ionic conductivity measurements to be completed. Finally, the degradability properties of CNC post-use in electronic applications with varying sulfur and NaCl concentrations must be characterized to learn more about the biodegradation of this material. These in-depth characterizations of CNC are necessary for ensuring this eco-friendly material is ready for real-world applications, such as wearable electronics, which is an application space inaccessible to traditional silicon-based devices.

MATERIALS AND METHODS

Substrate Preparation

A Kapton substrate was made hydrophobic by soaking in a 1M KOH (Sigma-Aldrich, Cat# 105033) solution for 3 minutes. Once removed from the KOH solution, the substrates were rinsed briefly with deionized (DI) water and dried with nitrogen.

Graphene Ink Preparation and Deposition

Graphene ink in water with a graphene concentration of 7% w/v (Sigma-Aldrich, Cat# 808261) was diluted with DI water to a graphene concentration of 2.33% w/v. The prepared graphene ink was printed with an Optomec AJ300 aerosol jet printer. A 150 μm printer nozzle was used at a printing speed of 2 mm/s. A sheath flow of 25 sccm, carrier gas flow range of 37 - 40 sccm, and an ultrasonic atomizer current of 350 mA were used to print the graphene at room temperature. A single pass was used to create the bottom and top capacitor contacts.

CNC Ink Preparation and Printing

CNC at a 10% w/v concentration in water (Cellulose Lab Inc, high sulfonic group content) was diluted with DI water to a CNC concentration 6% w/v. Specific amounts of NaCl were added to the DI water prior to diluting the CNC slurry to achieve the desired NaCl concentration of the ink. Utilizing the Optomec AJ300 aerosol jet printer, a 300 μm printer nozzle was used at a print speed of 5 mm/s. A sheath flow of 38 sccm, carrier gas flow of 30 sccm, and an ultrasonic atomizer current of 350 mA were used to print the CNC ink at room temperature. A single pass was used to create the dielectric layer of the capacitor.

Capacitor Fabrication

On a Kapton (polyimide) substrate, a 2.3 mm x 1.5 mm graphene bottom electrode was printed, followed by the CNC dielectric layer, and finally, the top graphene electrode, with the same electrode dimensions as the bottom contact. This formed a parallel-plate capacitor structure.

Instrumentation, Characterization, and Parameter Extraction

A scanning electron microscope (SEM) (Apreo S, ThermoFisher Scientific) was utilized to image the graphene and CNC surfaces. All electrical measurements of the capacitors were completed with a manual analytical probe station connected to an SMU (Keysight B2902A). The charging current was extracted from the peak current when

switching between voltages. The RC value was the time at which the current decreased to 33% of the peak current after switching between applied voltages. The charging current and RC values were averaged over two charging and discharging cycles.

ACKNOWLEDGEMENTS

We would like to acknowledge all members of the Franklin group, including Faris Albarghouthi, Brian Cole, Jay Doherty, Hansel Alex Hobbie, Brittani Huegen, Shiheng Lu, Alexander Mangus, Baiyu Zhang, Rubi Vazquez, and Iman Khanani, for their support of this work and sharing their insights into college and engineering with Elizabeth. The SEM images were obtained at the Duke University Shared Materials Instrumentation Facility (SMIF), a member of the North Carolina Research Triangle Nanotechnology Network (RTNN), which is supported by the National Science Foundation (grant no. ECCE-1542015) as part of the National Nanotechnology Coordinated Infrastructure (NNCI). This work was supported by the National Institutes of Health (1R01HL146849) and the National Science Foundation via Graduate Research Fellowship (Grant No. 2139754).

Received: October 3, 2022

Accepted: February 1, 2023

Published: August 16, 2023

REFERENCES

1. Mack, Chris. "The Multiple Lives of Moore's Law." *IEEE Spectrum*, vol. 52, no. 4, 2015, pp. 31–37, <https://doi.org/10.1109/MSPEC.2015.7065415>.
2. Shalf, John. "The Future of Computing beyond Moore's Law." *Philosophical Transactions of the Royal Society A: Mathematical, Physical and Engineering Sciences*, vol. 378, no. 2166, 2020, p. 20190061, <https://doi.org/10.1098/rsta.2019.0061>.
3. He, Zihan. "Analysis on the Development of Semiconductor Manufacturing Process." *Journal of Physics: Conference Series*, vol. 2295, no. 1, 2022, p. 012009, <https://doi.org/10.1088/1742-6596/2295/1/012009>.
4. US.EPA. "Sector Spotlight: Electronics." United States Environmental Protection Agency: EPA Center for Corporate Climate Leadership, 2021, <https://www.epa.gov/climateleadership/sector-spotlight-electronics>.
5. Irimia-Vladu, Mihai, et al. "Green and Biodegradable Electronics." *Materials Today*, vol. 15, no. 7–8, 2012, pp. 340–46, [https://doi.org/10.1016/S1369-7021\(12\)70139-6](https://doi.org/10.1016/S1369-7021(12)70139-6).
6. Franklin, Aaron D. "Nanomaterials in Transistors: From High-Performance to Thin-Film Applications." *Science*, vol. 349, no. 6249, 2015, p. aab2750, <https://doi.org/10.1126/science.aab2750>.
7. Williams, Nicholas X., et al. "Printable and Recyclable Carbon Electronics Using Crystalline Nanocellulose Dielectrics." *Nature Electronics*, vol. 4, no. 4, Apr. 2021, pp. 261–68, <https://doi.org/10.1038/s41928-021-00574-0>.
8. Huang, Wei, et al. "Dielectric Materials for Electrolyte Gated Transistor Applications." *Journal of Materials*

- Chemistry C*, vol. 9, no. 30, 2021, pp. 9348–76, <https://doi.org/10.1039/d1tc02271g>.
9. Bacakova, Lucie, et al. “Versatile Application of Nanocellulose: From Industry to Skin Tissue Engineering and Wound Healing.” *Nanomaterials*, vol. 9, no. 2, 2019, <https://doi.org/10.3390/nano9020164>.
 10. Hoeng, Fanny, et al. “Use of Nanocellulose in Printed Electronics: A Review.” *Nanoscale*, vol. 8, no. 27, 2016, pp. 13131–54, <https://doi.org/10.1039/c6nr03054h>.
 11. Wang, Shuangyuan, et al. “Preparation and Recycling of High-Performance Carbon Nanotube Films.” *ACS Sustainable Chemistry and Engineering*, vol. 10, no. 12, 2022, pp. 3851–61, <https://doi.org/10.1021/acssuschemeng.1c07089>.
 12. Li, Jinhua, et al. “Solution-Processable Organic and Hybrid Gate Dielectrics for Printed Electronics.” *Materials Science and Engineering R: Reports*, vol. 127, 2018, pp. 1–36, <https://doi.org/10.1016/j.mser.2018.02.004>.
 13. Cardenas, Jorge A., et al. “In-Place Printing of Flexible Electrolyte-Gated Carbon Nanotube Transistors with Enhanced Stability.” *IEEE Electron Device Letters*, vol. 42, no. 3, 2021, pp. 367–70, <https://doi.org/10.1109/led.2021.3055787>.
 14. Schroder, Dieter K. “Semiconductor Material and Device Characterization: Third Edition.” *Semiconductor Material and Device Characterization: Third Edition*, 3rd ed., John Wiley & Sons, 2005, <https://doi.org/10.1002/0471749095>.
 15. Torrisi, Felice, et al. “Inkjet-Printed Graphene Electronics.” *ACS Nano*, vol. 6, no. 4, Mar. 2012, pp. 2992–3006, <https://doi.org/10.1021/nn2044609>.

Copyright: © 2023 Franklin, Smith, and Franklin. All JEI articles are distributed under the attribution non-commercial, no derivative license (<http://creativecommons.org/licenses/by-nc-nd/3.0/>). This means that anyone is free to share, copy and distribute an unaltered article for non-commercial purposes provided the original author and source is credited.